Research Square

Preprints are preliminary reports that have not undergone peer review.
They should not be considered conclusive, used to inform clinical practice,
or referenced by the media as validated information.

Self-Position Control of Unmanned Vehicle Using Online System Identification

Ehab Safwat

e.khattab@mtc.edu.eg

Military Technical College, Egyptian Armed Forces

Ahmed Nasr Ouda

Egyptian Armed Forces

Amr Mohamed

Egyptian Armed Forces

Article

Keywords: Recursive Least-Square, System Identification, self-tuning, adaptive

Posted Date: November 11th, 2026

DOI: https://doi.org/10.21203/rs.3.rs-11400768/v1

License: This work is licensed under a Creative Commons Attribution 4.0 International License.
Read Full License

Additional Declarations: No competing interests reported.

Self-Position Control of Unmanned Vehicle Using Online System Identification

Ehab Safwat[1*], A. N. Ouda[2] and Amr Mohamed[2]

[1]Military Technical College, Egyptian Armed Forces, Egypt.
[2]Technical Research Center, Egyptian Armed Forces, Egypt.

*Corresponding author(s). E-mail(s): e.khattab@mtc.edu.eg;
Contributing authors: Ahnasroda@yahoo.com;
Amr.mohamed@ontariotechu.net;

Abstract

This paper presents a real-time system identification method for unmanned ground vehicle (UGV) using a System Identification (SI) approach. The online System Identification approach is introduced to select and estimate the significant parameters of unmanned systems, thereby enhancing the dynamic performance of an adaptive control system. The technique is demonstrated using a rover vehicle. A Recursive-Least-Square (RLS) algorithm is applied to estimate the unknown parameters. Additionally, a self-position controller based on continuous estimation of rover parameters is designed and evaluated. The simulation results show that the developed model using SI satisfies the rover model. Moreover, the developed self-position controller has a high performance.

Keywords: Recursive Least-Square, System Identification, self-tuning, adaptive

1 Introduction

Unmanned ground vehicles (UGVs) are expected to replace humans in a wide range of applications due to their numerous advantages in both civil and military domains, including rescue missions and surveillance operations. Consequently, the UGV autopilot is considered one of the most critical parts. However, developing an effective autopilot is a complex task, as it involves managing numerous interdependent variables that must be carefully considered and addressed [1].

The importance of the mathematical model is considered a critical part in the development, so the autopilot modelling attracted great attention due to high-reliability validated mathematical models. Modelling of such systems mainly relies on two main approaches, the physics-based technique and the system identification (SI) technique. In the system identification (SI) approach, the unmanned ground vehicle (UGV) is treated as a whole system. It relies on real-world maneuvers during which input and output data are recorded. Based on this data, a validated model of the underlying system can be estimated [2] as discussed in [3–7].

SI is particularly effective in addressing significant problem especially in the field of autonomous systems. This approach was introduced to investigate the performance of the system. Consequently, the system model can be estimated by monitoring its input/output signals [8]. The underlying system can be accurately defined by analyzing the relationship between the input and output data, for example kinematic modelling and the calibration of robotic systems [9–13]; parameter identification [14–17], NN-based SI [18–22]. and the prediction of the environment [23].

The design of controllers for unmanned ground vehicles (UGVs) has been widely investigated in numerous studies. For example, advanced control techniques such as Model Predictive Control (MPC) and adaptive control have proven effective in addressing the complexities of such systems leveraging human expertise about system dynamics [24–26]. Moreover, these controllers offer the advantages of efficient computation time and improved system performance, as demonstrated by Ouda [27].

Closed loop identification algorithms are direct, indirect and joint input-output as introduced by [28, 29]. Therefore, in this paper, each algorithm will be discussed in addition to appropriate system identification techniques used for implementation.

In the first direct approach, both the input and output of the system are measured, as illustrated in Fig. 1. In this configuration, no feedback is applied. The main advantage is that there is no need for system knowledge [30–33].

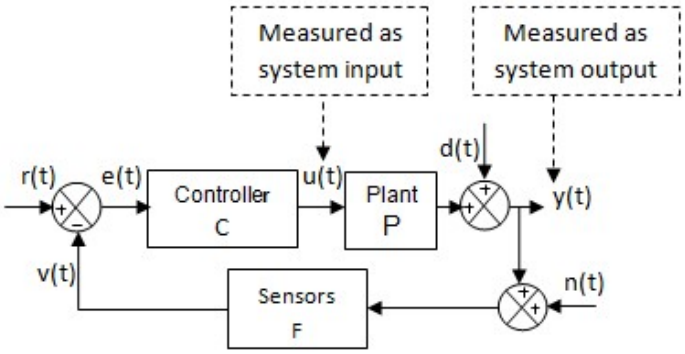


Fig. 1: Direct approach

The second closed-loop approach considers the indirect approach as shown in Fig. 2. In this case, the closed loop system G_{cl} can be estimated using the measured input and output. Thus, the TF of plant P can be estimated using the form $G_{cl} = \frac{C \cdot G}{1 + C \cdot G \cdot F}$ [34].

The third approach is the joint input-output, as shown in Fig. 3; this SI method can be obtained as follows: $y \begin{pmatrix} y \\ u \end{pmatrix} = Ar + Bn$ where A is comprised of two models, G_{cl} is the closed loop model. Subsequently, the model P can be obtained using this form, $P = \frac{G_{cl}}{G_{ru}}$.

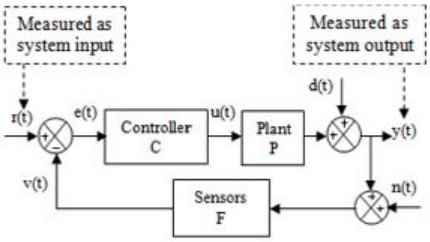


Fig. 2: Indirect approach

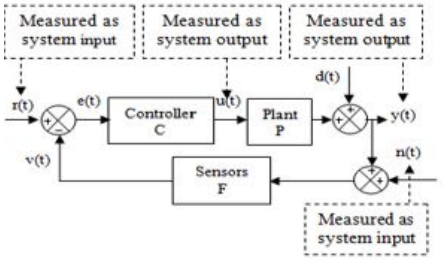


Fig. 3: Joint input-output approach

This paper discussed the development of online closed-loop technique for estimating the model parameter of UGV along with the implementation of an adaptive control scheme. The input/output signals of the UGV are thoroughly verified and evaluated. Subsequently, a Fuzzy Logic Controller (FLC) is implemented to effectively control the UGV, ensuring dynamic and robust performance.

2 Remotely Operated Vehicle

A remotely operated UGV shown in Fig. 4 was developed in the robotics lab at the University of Carleton. It utilizes the Romeo microcontroller; an all-in-one platform specifically designed for robotics to facilitate easy development of open-source robotic applications.

(DFRduino) provides many advanced versions of the Romeo controller. The version used for this experiment is "DFRduino Romeo V1.0". Fig. 5 shows a glimpse of the controller.

2.1 Motor Control System (MCS)

The Arduino Romeo robotic controller is an open-source platform that features a dedicated motor power supply and a bidirectional DC motor driver. The separate motor power supply is specifically designed to provide power exclusively to the motor controllers, thereby ensuring that other devices, such as the ATmega328 microprocessor, receive an independent and stable power source. The schematic of the motor control pin jumpers and the motor DC outputs is shown in Fig. 6.

In Fig. 7, the gray and the orange cables go to motor 2 on the left and the gray and the black cables go to motor 1 on the right. These motors were controlled by passing a value in the range of 0:200. The passed value denotes the frequency-to-input-voltage ratio.

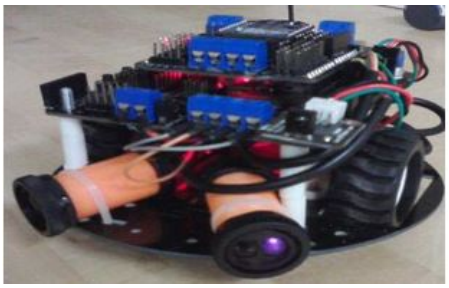


Fig. 4: Remotely Operated Vehicle

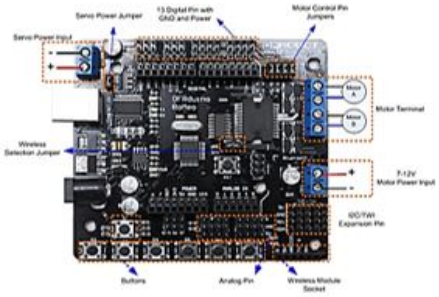


Fig. 5: (DFRduino) Robotic microcontroller



Fig. 6: Motor control jumpers and pins

2.2 Accelerometer – Robot Assembly

To achieve obstacle avoidance and position control for the developed robot, an accelerometer was installed as shown in Fig. 8, to measure the instantaneous acceleration along the three coordinates (X, Y and Z). The acceleration data is integrated to obtain instantaneous velocity and then integrated again to determine the corresponding position. A Kalman filter was applied to enhance the azimuthal data in the yaw plane, effectively reducing noise and improving measurement precision.

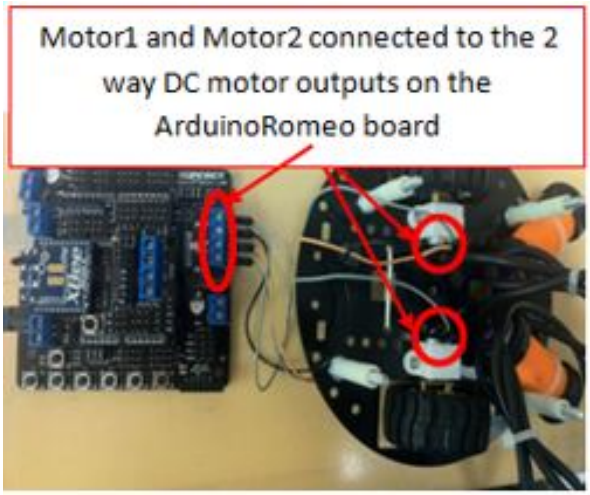


Fig. 7: Motor Control connection system on the Arduino Romeo robotic board

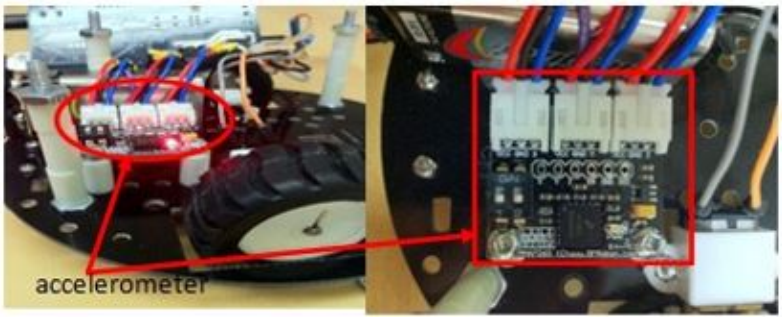


Fig. 8: Accelerometer – Robot assembly

3 Offline Open Loop (OL) System Identification

System identification (SI) is a methodology used to model the dynamics of a system based on i/o data obtained through experimental investigation. SI is able to build mathematical model of dynamical system. SI has five steps that should follow in order to estimate the system models.

SI using parametric identification algorithm model structure is illustrated in (1). These parameters can be estimated by monitoring the i/o data. Furthermore, this algorithm is able to provide a large variety of describing the underlying system dynamics, where Y(Z) is defined as follows.

$$Y(z) = G(z)X(z) + M(z) \tag{1}$$

Consequently, (1) can be rewritten as in (2); where $Y(z)$ is the n_y output, $X(z)$ is the n_x input, $E(z)$ is the transformation of a white noise $\in (t)$, $G(z)$ is the transfer

function of the system, and $H(z)$ is the stochastic behavior of noise.

$$Y(z) = G(z)\ X(z) + H(z)E(z) = (N(z))/(D(z))X(z) + (A(z))/(B(z))E(z) \quad (2)$$

UGV model can be estimated by applying different estimation models. For this experiment, the best fitted model output is obtained by Auto Regressive with Exogenous Input (ARX) model.

The ARX model described in (3) is the simplest estimation model as shown in Fig. 9. The main disadvantage of this model is the disturbance model (1/N(z)). Consequently, this issue can be solved by higher orders coefficients of terms A, B, where the signal to noise ratio is acceptable.

$$D(z)Y(z) = N(z)X(z) + E(z) \quad (3)$$

Several experiments were conducted using different input values to estimate the plant transfer function with the ARX model. In this approach, the input was defined as the frequency-to-voltage ratio, while the output corresponded to the instantaneous velocity obtained by integrating the acceleration measured from the accelerometer. The experimental setup, illustrated in Fig. 10, was used to estimate the open-loop plant dynamics, which include the motor, gears, robot structure, and sensors.

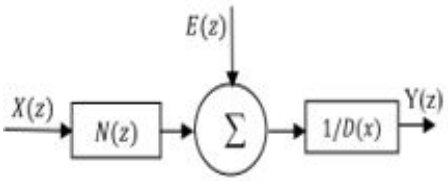


Fig. 9: ARX model

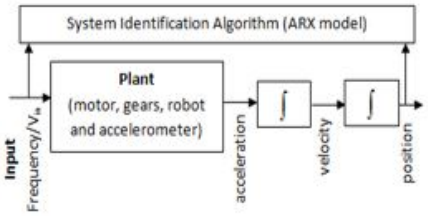
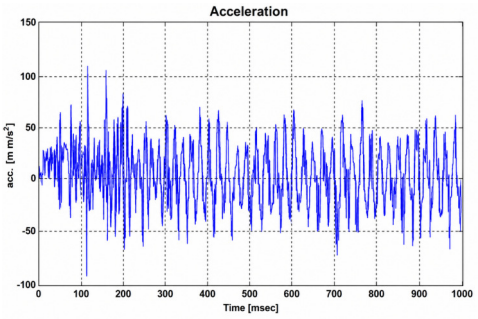


Fig. 10: OL Experiment

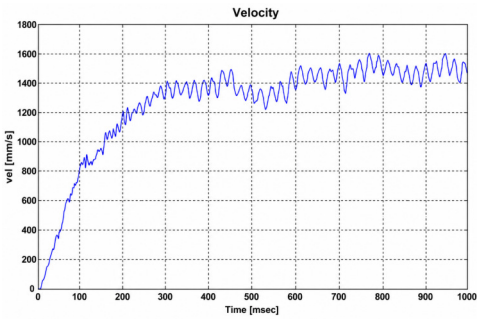
Sample results are illustrated. This sample experiment is done in one second via input frequency in a ratio to the input voltage equal 200. The obtained acceleration, velocity, and position in inches are illustrated in Fig. 11. The velocity profile clarifies that the transfer function concerning velocity to input relation is best expressed as first order transfer function. Fig. 12 concerning the open loop transfer function reveals the same result. The obtained plant transfer function can be illustrated in (4).

$$\frac{velocity}{input} = \frac{61.49}{s + 8.619} \quad (4)$$

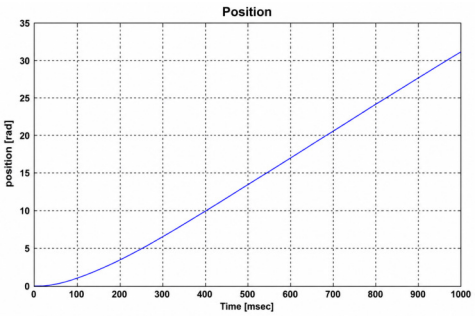
The same experiment has been repeated via input frequency in a ratio to the input voltage equal 150, 100 and 50. The step response of the estimated plant models from sampled experiments is shown in Fig. 13 which clarifies that the estimated plant



(a) Acceleration



(b) Velocity



(c) Position

Fig. 11: Open Loop Experiment Results ((a) Acceleration, (b) Velocity, (c) Position)

transfer functions from sampled experiments have nearly the same response and the estimated transfer function via 1st experiment.

4 Recursive Least Square Online Estimation

Assuming the system described by the (SISO) system:

$$A(z^{-1})y(t) = B(z^{-1})(u(t-d_0) + v(t-d_0)) \tag{5}$$

where$A(z^{-1}) = 1 + a_1 z^{-1} + ... + a_n z^{-n}$ and $B(z^{-1}) = b_0 + b_1 z^{-1} + ... + b_m z^{-m}$, $m = n - d_0$, y is the output, u is the input of the system, and v is a disturbance.

The least-square technique is widely employed in SI. The methodology minimizes the sum of squares differences between observed and predicted values in order to select the unknown parameters of the mathematical model. The derivation of the analytic solution is discussed in [35]. Consequently, real time data observation is obtained sequentially. In addition, the recursive estimation algorithm minimizes the computational time using obtained results at time t to get the estimation at time t+1. Therefore, RLS estimation method is introduced. The process model in (5) can be written as follows:

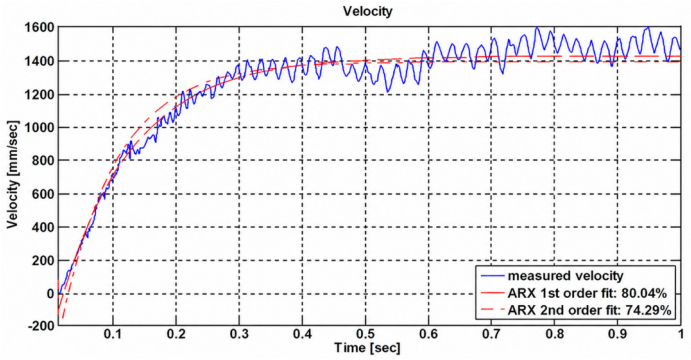


Fig. 12: Measured Velocity and Estimated ARX Models

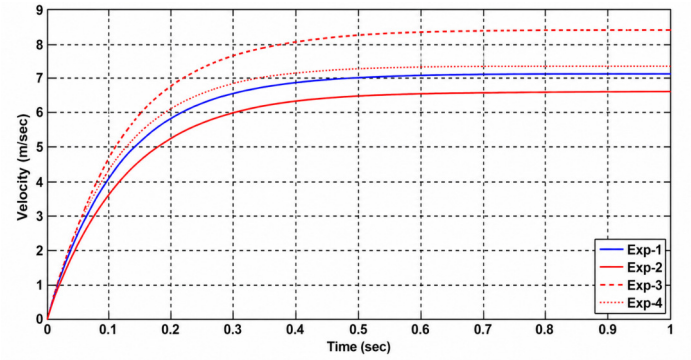


Fig. 13: Estimated Plant Step Response

$$y(k) = -a_1 y(k-1) - a_2 y(k-2) - ..... - a_n y(k-n) + b_0 u(k-d_0) + ... + b_m u(k-d_0-m) \tag{6}$$

Due to the linearity of the model parameters, therefore, we obtained the following form:

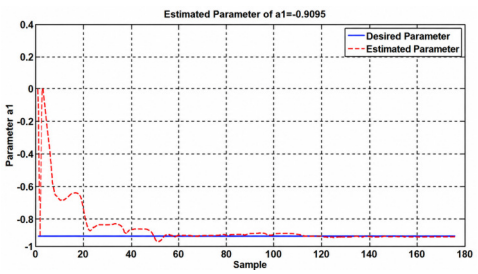
$$y(k) = \phi^T(k)\theta \tag{7}$$

where $\theta = [b_0, b_1, .., b_m, a_1, a_2, .., a_n]^T$, $\phi(k) = [u(k-d_0), .., u(k-d_0-m), -y(k-1), .., -y(k-n)]^T$. The recursive least square estimator is given by:

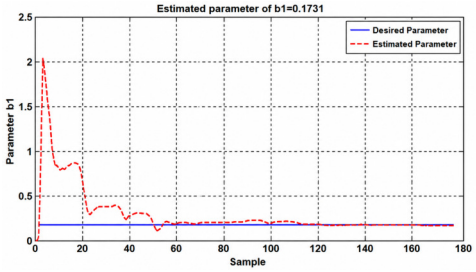
$$\begin{aligned} \hat{\theta}(k) &= \hat{\theta}(k-1) + K(k)\left[v(k) - \varphi^T(k)\hat{\theta}(k-1)\right] \\ K(k) &= P(k-1)\varphi(k)\left(I + \varphi^T(k)P(k-1)\varphi(k)\right)^{-1} \\ P(k) &= P(k-1) - P(k-1)\varphi(k)\left[I + \varphi^T(k)P(k-1)\varphi(k)\right]^{-1}\varphi^T(k)P(k-1) \end{aligned} \tag{8}$$

4.1 Closed Loop Estimation

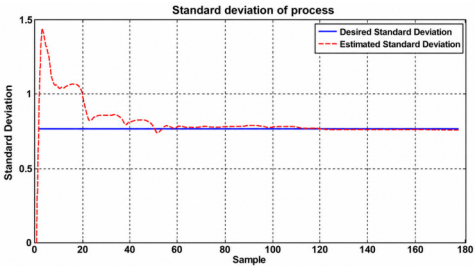
The experiment described in Section 3 will be repeated for a closed-loop plant. An offline system identification procedure based on the ARX model will then be applied to determine the plant's transfer function. The estimated robot transfer function for all the experiment period can be considered as $\frac{v(s)}{in(s)} = \frac{90.74}{s+47.43}$ which can be represented in discrete form as $\frac{v(z)}{in(z)} = \frac{0.1731}{z-0.9095}$. Then, applying a recursive least square method for the whole data extracted from a closed loop experiment, the obtained results will be shown in Figs 14–16.



(a) a_1 Parameter



(b) b_1 Parameter



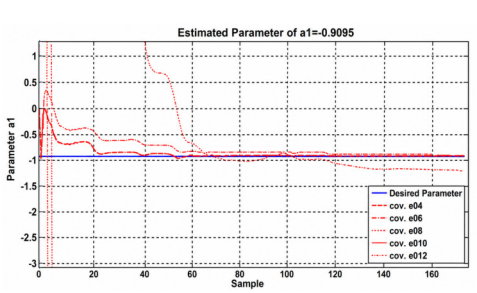
(c) Standard Deviation

Fig. 14: Closed Loop (CL) Experiment

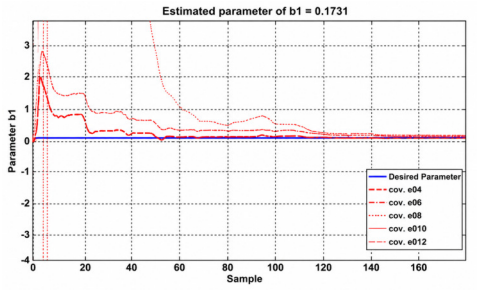
Finally, the estimated plant dynamics has a discrete form as $\frac{v(z)}{in(z)} = \frac{0.1659}{z-0.9122}$ which can be represented in continuous form as $\frac{v(s)}{in(s)} = \frac{86.81}{s+45.97}$. This is a coincidence with estimated one via off-line experiment expressed earlier in this section.

4.2 Effect of Varying the Covariance Matrix

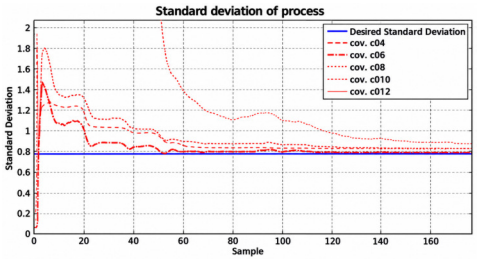
The effect of the covariance matrix is illustrated in Fig. 15. It shows that the covariance matrix has a slight influence on the convergence rate of the estimated parameters, but this effect remains within a certain limit. In this experiment, when the covariance matrix was increased beyond this limit $p_o = 1X10^{12}$ the process became unstable. The obtained results can be summarized as follows:



(a) a_1 Parameter



(b) b_1 Parameter



(c) Standard Deviation

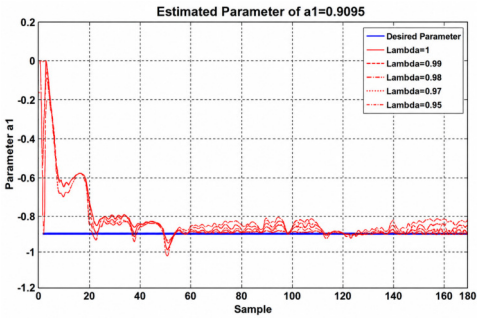
Fig. 15: CL with varying covariance matrix

Table 1: CL with a varying Covariance matrix

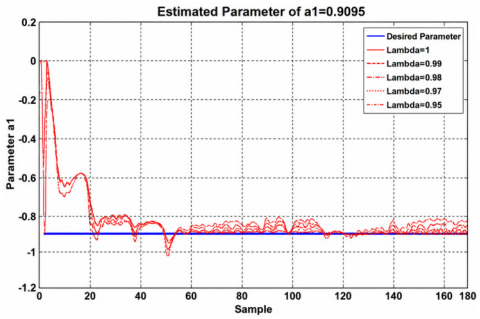
Covariance matrix		$[p_o = 1X10]$	$[p_o = 1X10^6]$	$[p_o = 1X10^9]$	$[p_o = 1X10^{12}]$	$[p_o = 1X10^{15}]$
Parameter a_1	Desired	-0.9095	-0.9095	-0.9095	-0.9095	-0.9095
	Obtained	-0.9085	-0.9089	-0.9092	Unstable	Unstable
Parameter b_1	Desired	0.1731	0.1731	0.1731	0.1731	0.1731
	Obtained	0.1723	0.1727	0.1729	Unstable	Unstable
Standard Deviation	Desired	0.79	0.79	0.79	0.79	0.79
	Obtained	0.785	0.786	0.789	Unstable	Unstable

4.3 Effect of Varying the Forgetting Factor

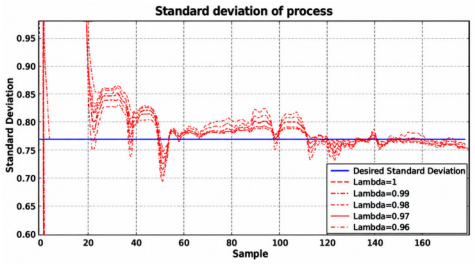
The effect of decreasing the covariance matrix and the corresponding results are shown in Fig. 16. The figure illustrates that reducing the covariance matrix influences the convergence rate of the estimated parameters, but this effect remains within a specified limit. In this experiment, when the forgetting factor was decreased to 0.8, the process became unstable.



(a) a_1 Parameter



(b) b_1 Parameter



(c) Standard Deviation

Fig. 16: CL with varying forgetting factor

Table 2: OL with a varying forgetting factor

Forgetting factor		$[\lambda = 1$	$\lambda = 0.9$	$\lambda = 0.8$	$\lambda = 0.7$	$\lambda = 0.6$	
Parameter a_1	Convergence Sample		62	58	Unstable	Unstable	Unstable
Parameter b_1	Convergence Sample		65	60	Unstable	Unstable	Unstable
Standard Deviation	Convergence Sample		73	69	Unstable	Unstable	Unstable

5 Self-Position Control

Considering the closed-loop experiment illustrated in Fig. 17, the estimated plant encompassing the motor, gearbox, robot, and accelerometer is represented by $\frac{velocity}{input} = \frac{61.49}{s+8.619}$. The gain ratio used to convert the raw measured position into its equivalent value in meters is defined by $gain \approx 0.025$.

Two simple controllers are designed, one is a fixed controller, and the other is a gain scheduling self-position controller. The comparative study is presented in the next subsection to emphasize the benefits of online system identification used in self-position controller.

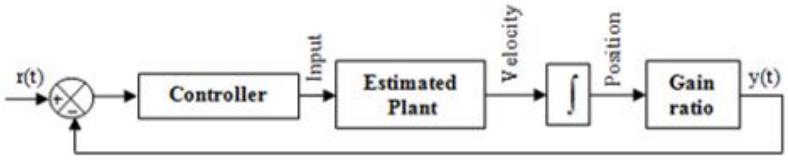


Fig. 17: Closed Loop Experiment

5.1 Design of Fixed Controller

The controller is designed as a proportional controller with gain k. The closed-loop transfer function can be expressed as $\frac{y}{r} = \frac{1.53725K}{s^2+8.619s+1.53725K}$. By comparing the coefficients of this transfer function with those of the standard second-order system, given by $\frac{\omega^2}{s^2+2\zeta\omega s+\omega^2}$, the desired damping ratio is determined, which in turn yields the corresponding natural frequency $\omega \approx 3.747$ and the resulting controller gain, as shown in ($K \approx 9.135$).

5.2 Design of Self-Position Controller

The Self-Tuning Regulator (STR) can be regarded as an identifier-based adaptive controller, as illustrated in Fig. 18. The block labeled "Estimator" performs online estimation of the process parameters using least squares method. The block labeled "Controller design" represents the online computation of a control law based on either known or estimated parameters, producing a controller that is implemented within the feedback loop. The system can be observed as an automation of processing modelling/estimation and design, in which the process model and the control design are updated at each sampling interval.

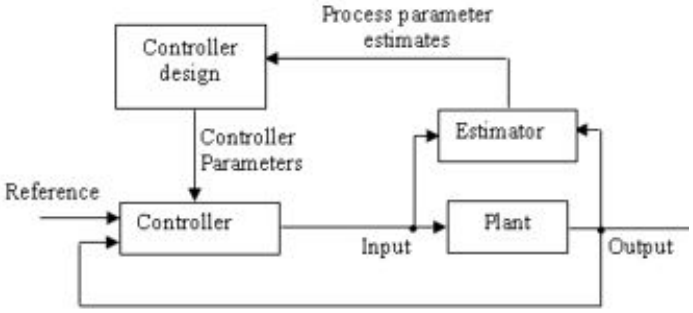


Fig. 18: Block diagram of Self position regulator

The designed controllers were implemented in a real experiment with the desired position to be 12 [m]; the results are shown in Fig. 19.

The above results clarify that the designed self-position controller has a good performance and lower steady state error compared to classical one.

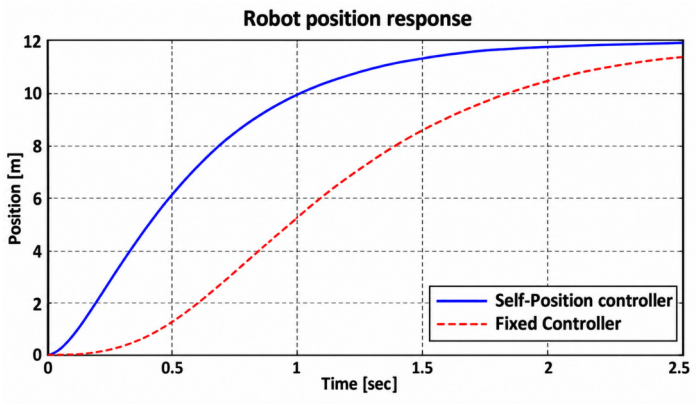


Fig. 19: Robot Position response

6 Conclusion

In this paper, the theory of real-time system identification has been successfully applied to select and estimate the key parameters of an unmanned vehicle. By implementing offline closed-loop control, an accurately identified model can be obtained as the initial covariance matrix increases. Moreover, when the forgetting factor decreases, the convergence rate of the estimated parameters increases up to a certain point, beyond which oscillations appear in the steady-state phase. Consequently, the initial covariance matrix in the adaptive structure should be defined in the form of $p_o = 1X10^6$ to minimize these oscillations. Furthermore, the suitable range for selecting the forgetting factor is between 0.92 and 1.

Field deployments were conducted to validate the proposed system identification technique. When compared to the results from offline identification methods involving numerical optimization, the online estimates perform favourable. Subsequently, a self-positioning controller was developed and evaluated, which relies on the continuous estimation of rover parameters. The obtained results demonstrate the effectiveness of online system identification, showing that the designed self-position controller achieves higher performance and reduced steady-state error compared to the classical controller.

Funding

Open access funding provided by The Science, Technology & Innovation Funding Authority (STDF) in cooperation with The Egyptian Knowledge Bank (EKB). The corresponding author is affiliated with the Military Technical College (MTC), which is covered under the STDF agreement with *Scientific Reports*. This research received no specific grant from any funding agency in the public, commercial, or not-for-profit sectors.

Author Contributions

Ehab Khattab: Conceptualization, Methodology, Software, Validation, Formal analysis, Investigation, Data curation, Writing – original draft, Writing – review & editing, Visualization. He conceived and designed the study, developed the online system identification framework based on the Recursive Least-Squares (RLS) algorithm, implemented the ARX model structure for both open-loop and closed-loop estimation, designed the self-tuning regulator (STR) and fixed proportional controller, performed the covariance matrix and forgetting factor sensitivity analyses, and drafted the manuscript.

Ahmed Oda: Methodology, Software, Investigation, Resources, Validation, Writing – review & editing. He contributed to the development and assembly of the remotely operated UGV platform (DFRduino Romeo V1.0 microcontroller, motor control system, and accelerometer integration), conducted the experimental data acquisition campaigns, and assisted in the offline/online identification experiments and the interpretation of results.

Amr Mohamed: Supervision, Conceptualization, Methodology, Formal analysis, Writing – review & editing, Project administration. He supervised the research, provided technical guidance on the closed-loop identification approaches (direct, indirect, and joint input–output), advised on the adaptive control design and stability considerations, and critically reviewed and edited the manuscript.

All authors read and approved the final manuscript.

References

[1] RIBLER, R.L., J.S. VETTER, H. SIMITCI and D.A. REED. Autopilot: Adaptive Control of Distributed Applications. In: Proceedings of the Seventh International Symposium on High Performance Distributed Computing. Chicago: IEEE, 1998, pp. 172-179. DOI 10.1109/HPDC.1998.709970.

[2] OUDA, A.N. Performance Investigation of Adaptive Guidance Algorithms and Its Effectiveness [Ph.D. thesis]. Cairo: Military Technical College, 2012.

[3] ÅSTRÖM, K.J. and P. EYKHOFF. System Identification – a Survey. Automatica, 1971, 7(2), pp. 123-162. DOI 10.1016/0005-1098(71)90059-8.

[4] ENG, Y.H., K.M. TEO, M. CHITRE and K.M. NG. Online System Identification of an Autonomous Underwater Vehicle via In-Field Experiments. IEEE Journal of Oceanic Engineering, 2016, 41(1), pp. 5-17. DOI 10.1109/JOE.2015.2403576.

[5] LAI, Y.-C. and Q.L. TRI. System Identification and Control of a Small Unmanned Helicopter at Hover Mode. In: 2017 2nd International Conference on Control and Robotics Engineering (ICCRE). Bangkok: IEEE, 2017. DOI 10.1109/ICCRE.2017.7935049.

[6] OUDA, A.N., A. MOHAMED, M. EL-GINDY, H. LANG, and J. REN. Development and Modelling of Remotely Operated Scaled Multi-Wheeled Combat

Vehicle Using System Identification. International Journal of Automation and Computing, 2019, 16(2). DOI 10.1007/s11633-018-1161-8.

[7] KUMAR, N., S. SADERLA and Y. KIM. System Identification of Cropped Delta UAVs from Flight Test Methods Using Particle Swarm-Optimisation-Based Estimation. The Aeronautical Journal, 2023, 127(1307), pp. 76-96. DOI 10.1017/aer.2022.46.

[8] REYNDERS, E. System Identification Methods for (Operational) Modal Analysis: Review and Comparison. Archives of Computational Methods in Engineering, 2012, 19, pp. 51-124. DOI 10.1007/s11831-012-9069-x.

[9] Wang, Jianqi, Long, Shengtao, Wang, Su, Zhan, Kaiyu, Research on the Design and Simulation of Missile Intelligent Agent Autopilot Integrated With Deep Reinforcement Learning, International Journal of Aerospace Engineering, 2025, 9542576, 14 pages, 2025. https://doi.org/10.1155/ijae/9542576

[10] G. Chen et al., "Modeling and Control of General Hydraulic Excavator for Human-in-the-loop Automation," 2023 IEEE 35th International Conference on Tools with Artificial Intelligence (ICTAI), Atlanta, GA, USA, 2023, pp. 708-716, doi: 10.1109/ICTAI59109.2023.00110.

[11] RANÓ, I. and R. IGLESIAS. Application of Systems Identification to the Implementation of Motion Camouflage in Mobile Robots. Autonomous Robots, 2016, 40(2), pp. 229-244. DOI 10.1007/s10514-015-9449-9.

[12] RAPTIS, I.A., K.P. VALAVANIS and W.A. MORENO. System Identification and Discrete Nonlinear Control of Miniature Helicopters Using Backstepping. Journal of Intelligent & Robotic Systems, 2009, 55(2), pp. 223-243. DOI 10.1007/s10846-008-9295-5.

[13] WEST, C., A. MONTAZERI, S.D. MONK, D. DUDA and C.J. TAYLOR. A New Approach to Improve the Parameter Estimation Accuracy in Robotic Manipulators Using a Multi-Objective Output Error Identification Technique. In: 2017 26th IEEE International Symposium on Robot and Human Interactive Communication (RO-MAN). Lisbon: IEEE, 2017, pp. 1406-1411. DOI 10.1109/ROMAN.2017.8172488.

[14] ABDULSADDA, A.T. and K. IQBAL. An Improved SPSA Algorithm for System Identification Using Fuzzy Rules for Training Neural Networks. International Journal of Automation and Computing, 2011, 8, pp. 333-339. DOI 10.1007/s11633-011-0589-x.

[15] WILENSKY, R. An Extensive Review on Generator Excitation System Modelling, Design, and Parameter Identification [online]. [viewed 2024-01-09]. Available from: https://hal.science/hal-01352217/file/Excitation.pdf

[16] DING, F. Combined State and Least Squares Parameter Estimation Algorithms for Dynamic Systems. Applied Mathematical Modelling, 2014, 38(1), pp. 403-412. DOI 10.1016/j.apm.2013.06.007.

[17] JING, S.X., T.H. PAN and Z.M. LI. Recursive Bayesian Algorithm for Identification of Systems with Non-Uniformly Sampled Input Data. International Journal of Automation and Computing, 2018, 15(3), pp. 335-344.

[18] MOUSAVIAN, S.H. and H.R. KOOFIGAR. Identification-Based Robust Motion Control of an AUV: Optimized by Particle Swarm Optimization Algorithm. Journal of Intelligent & Robotic Systems, 2017, 85(2), pp. 331-352. DOI 10.1007/s11633-017-1073-z.

[19] WU, X.J., X.L. WU and X.Y. LUO. Adaptive Neural Network Dynamic Surface Control for a Class of Nonlinear Systems with Uncertain Time Delays. International Journal of Automation and Computing, 2016, 13(4), pp. 409-416. DOI 10.1007/s11633-015-0945-3.

[20] ORTEGA, R. and M.W. SPONG. Adaptive Motion Control of Rigid Robots: A Tutorial. Automatica, 1989, 25(6), pp. 877-888. DOI 10.1016/0005-1098(89)90054-X.

[21] MORADI, M. and H. MALEKIZADE. Neural Network Identification Based Multivariable Feedback Linearization Robust Control for a Two-Link Manipulator. Journal of Intelligent & Robotic Systems, 2013, 72, pp. 167-178. DOI 10.1007/s10846-013-9827-5.

[22] NOËL, J.P. and G. KERSCHEN. Nonlinear System Identification in Structural Dynamics: 10 More Years of Progress. Mechanical Systems and Signal Processing, 2017, 83, pp. 2-35. DOI 10.1016/j.ymssp.2016.07.020.

[23] HAVERKAMP, B.R.J., C.T. CHOU, M.H. VERHAEGEN and R. JOHANSSON. Identification of Continuous-Time MIMO State Space Models from Sampled Data, in the Presence of Process and Measurement Noise. In: Proceedings of 35th IEEE Conference on Decision and Control. Kobe: IEEE, 1996, pp. 1539-1544. DOI 10.1109/CDC.1996.572741.

[24] HE, S., X. XU, J. XIE, F. WANG and Z. LIU. Adaptive Control of Dual-Motor Autonomous Steering System for Intelligent Vehicles via Bi-LSTM and Fuzzy Methods. Control Engineering Practice, 2023, 130, 105362. DOI 10.1016/j.conengprac.2022.105362.

[25] ZHOU, X., Z. WANG, H. SHEN and J. WANG. Robust Adaptive Path-Tracking Control of Autonomous Ground Vehicles with Considerations of Steering System Backlash. IEEE Transactions on Intelligent Vehicles, 2022, 7(2), pp. 315-325. DOI 10.1109/TIV.2022.3146085.

[26] LAMOUIK, I., A. YAHYAOUI and M.A. SABRI. Model Predictive Control for Full Autonomous Vehicle Overtaking. Transportation Research Record: Journal of the Transportation Research Board, 2023, 2677(5), pp. 1193-1207. DOI 10.1177/0361198122114143

[27] OUDA, A.N., G.A. EL-SHEIKH, Y.Z. EL-HALWAGY and M. ASHRY. Nominal Model Selection and Guidance Computer Design for Antitank Guided Missile. International Journal of Automation and Control, 2019, 13(1), pp. 34-83. DOI 10.1007/s40435-017-0352-4.

[28] PRAMOD, S. and M. CHIDAMBARAM. Closed Loop Identification of Transfer Function Model for Unstable Bioreactors for Tuning PID Controllers. Bioprocess Engineering, 2000, 22, pp. 185-188. DOI 10.1007/s004499900077.

[29] ZHU, Y. and F. BUTIYI. Case Studies on Closed Loop Identification for MPC. Control Engineering Practice, 2002, 10(4), pp. 403-417. DOI 10.1016/S0967-0661(02)00007-2.

[30] SUN, L., H. OHMORI and A. SANO. Output Intersampling Approach to Direct Closed-Loop Identification. IEEE Transactions on Automatic Control, 2001, 46(12), pp.1936-1941. DOI 10.1109/9.975487.

[31] HELLGREN, J. Analysis of Feedback Cancellation in Hearing Aids with Filtered-x LMS and the Direct Method of Closed Loop Identification. IEEE Transactions on Speech and Audio Processing, 2002, 10(2), pp. 119-131. DOI 10.1109/89.985549.

[32] KARA, T. and I. EKER. Nonlinear Closed-Loop Direct Identification of a DC Motor with Load for Low Speed Two-Directional Operation. Electrical Engineering, 2004, 86, pp. 87-96. DOI 10.1007/s00202-003-0189-z.

[33] KLERK, E. A Laboratory Experiment to Teach Closed Loop System Identification. IEEE Transactions on Education, 2004, 47(2), pp. 276-283. DOI 10.1109/TE.2004.825524.

[34] ZHENG, W. A Modified Method for Closed Loop Identification Transfer Function Models. IEEE Transactions on Circuits and Systems, 2002, 49(4), pp. 556-562. DOI 10.1109/81.995678.

[35] LJUNG, L. System Identification, Theory for Users. 2nd ed. New York: Pearson Education, 1999. ISBN 0-13-244053-9.